

## **EXPERIMENTAL AND NUMERICAL INVESTIGATIONS OF CONCRETE FAILURE UNDER TRIAXIAL LOADING**

M.L. Wang and Z. Chen  
Department of Civil and Materials Engineering  
University of Illinois at Chicago  
Chicago, IL 60607  
U.S.A.

### **Abstract**

Experimental and numerical simulations are presented in order to define the failure mechanism of cementitious materials.

Triaxial tests on 95 mortar cylinders show there is a change in the failure plane orientation as confining pressure increases. The failure is characterized by a distinct failure surface or surfaces that change orientation from nearly vertical to angled as confinement increases. Cap blocks are used to relieve the friction between the platens and the specimens under triaxial loading. The same conclusion is obtained by numerical analysis that includes a realistic 3-dimensional meso-structure simulation. A modified Gauss point method is applied to guarantee the efficiency and accuracy of the finite element analyses. The Drucker-Prager criterion and the low tensile strength criterion are used to simulate the failure mechanism.

Key words: Triaxial test, random aggregate distribution, modified Gauss point, failure mechanisms

### **1 Introduction**

Triaxial tests have shown that the angle of the failure plane for geologic materials changes with increasing confining pressure (Wawersik, 1971; Murrell, 1965). However, no detailed data for concrete has shown that there is a similar relationship between the confinement and the change in the angle of

the principle failure plane. Palaniswamy (1972), commenting on triaxial tests on cement paste, mortar, and concrete, stated that two distinct modes of behavior were observed, specifically, a splitting failure at low confining pressures, and a crushing failure at large confining pressures. Zimmerman (1977) found that the failure plane is always parallel to the direction of maximum compressive stress. The apparatus used in his tests employed platens to apply lateral pressure to the specimens. These platens may have constrained the true failure modes of the specimens. Tests by Gerstle (1980), using several different loading devices, showed that boundary constraints from the use of platens for lateral loading inhibit transverse deformations.

In this paper, both experimental and numerical studies show changes in the orientation of the failure plane as confining pressure increases.

Experimentally, it is essential to relieve the friction between the platens since this friction severely affects the development of the failure mechanism and, consequently, its orientation. Moreover the failure is characterized by a distinct failure surface or surfaces that change orientation from nearly vertical to angled as confinement increases. The same conclusion is obtained by numerical analysis that includes a realistic 3-dimensional meso-structure simulation. A modified Gauss point method is applied to guarantee the efficiency and accuracy of the huge-scale finite element analyses (148,500 lattices). Based on comparison of the experimental and numerical results, the strength ratio between cement paste (including interface) and coarse aggregate is randomly distributed between 0.1 to 0.4. The Drucker-Prager criterion and the low tensile strength criterion are used to simulate the failure mechanism.

## **2 Experimental Technique**

Triaxial tests were performed with confining pressures ranging from 0 to 56 Mpa. A total of 95 cylinders were tested in triaxial compression. Evaluating the effect of the methods used to relieve friction between the load platens and the specimens was essential in this study.

### **2.1 Equipment Setup**

A behavioral science engineering laboratories 70 kpa triaxial test cell was used to apply the lateral confining pressure. The test cell had a pressure transducer that was used to monitor fluid pressure inside the cell. The axial load was applied with a universal testing machine.

Measurements Group, Inc., EA-06-500BL-350 strain gauges were used in 56% of the tests (Wang and Ruthland, 1995). Only load-displacement data

were recorded in the remaining tests. Axial load and displacement data were recorded on an X-Y plotter. Some of the test data were digitized and stored on an IBM-compatible personal computer using an analog to digital converter.

## **2.2 Specimen Preparation**

All triaxial specimens were prepared with a water/cement ratio between .42 and .47. The cement/aggregate ratio was .25 by weight. Superplasticizer, Friz-pak Supercizer 6, was added to increase the workability of the mixes .3% by weight of cement.

Seventy-five specimens measuring 5 cm in diameter by 10 cm in height were cast in three batches of 25. Twelve specimens 5 cm in diameter by 20 cm in height were cast in a separate batch.

Cap blocks were prepared to help relieve the friction between the platens and the specimens. The cap blocks were 5 cm in diameter and 1.3 to 2.5 cm thick. The mix design for the cap blocks was similar to that of the specimens except that the cement/aggregate ratio was increased to .4, the water/cement ratio was decreased to .35, and the amount of superplasticizer was increased to .5%. The goal was to produce a material with similar deformation properties but with a higher strength. The modulus and lateral extension ratio of the two materials were similar (within 5%), while the uniaxial strength of the cap blocks was 50% larger than the strength of the specimens.

All specimen and cap blocks were polished on a lap table containing a coarse grit (100) lap pad. The cylinders and cap blocks contained air voids on the surfaces that would tear the triaxial membranes. In order to protect the membranes the surface voids were filled with clay. Triaxial membranes were placed on the specimens.

Several methods of relieving the friction between the specimen and the platens were tested. Based on some preparing tests, cap blocks alone, cap blocks with grease, and cap blocks with polyethylene sheets, were used to relieve the friction. All the tests were performed at 0, 1.7, 3.5, 7.0, 14.0, 28.0, 42.0, and 56.0 Mpa, and they were conducted using a standard triaxial loading where the displacement was monotonically increased up to and past the peak load.

## **3 Mesostructure Simulation**

In meso- or micro-scopic studies, it is necessary to generate a realistic 3-

dimensional multiphase system consisting of cement paste and coarse aggregate, especially for concrete (Desiderio, 1996). This is because mechanical behaviors are determined by extremes in the local stresses, which have a close relationship with the distribution of cement pastes and coarse aggregates, as well as with aggregate sizes in the meso-structure simulation. Here, the Monte Carlo method (Hassold, 1996) is used to simulate the cylinder specimen measuring 5 cm in diameter and 10 cm in height.

Automatic mesh generation produced 148,500 lattices for the cylinder sample ( Fig. 1). Generally, that amount of lattices is necessary to reach a properly aggregated size of the given concrete specimen. A non-zero index, which corresponds to both the phase and orientation of the aggregate, is initialized to each lattice by a random function. In a 2-phase simulation ( $\alpha$  and  $\beta$ ), the sign of  $S_i$  indicates the phase present at that site, while the absolute value of  $S_i$  corresponds to the orientation of the grain in which the site is embedded. Sites with one or more different closest neighbors are interface sites, sites with only like nearest neighbors are interior sites. Total system energy is specified by assigning a positive energy to interface areas (or cement pastes) and zero energy to the interior sites (or coarse aggregates), which can be calculated via the Hamiltonian equation (Hockin, 1980)

$$H = \frac{1}{8} \sum_{i=1}^N \sum_{j=1}^Z \left\{ (J_{\alpha\alpha} + J_{\beta\beta} + 2J_{\alpha\beta}) [1 - \delta(S_i, S_j)] + (J_{\alpha\alpha} + J_{\beta\beta} - 2J_{\alpha\beta}) \text{Sign}(S_i) \text{Sign}(S_j) + (J_{\alpha\alpha} - J_{\beta\beta}) [\text{Sign}(S_i) + \text{Sign}(S_j)] \right\} \quad (1)$$

In equation (1),  $N$  is the total sites of system.  $Z$  is the number of neighbors of  $i^{\text{th}}$  site.  $\delta$  is the Kronecker delta function. 'Sign' is the sign function defined as  $\text{Sign}(S_i)$  equals 1 if  $S_i$  is positive, and  $\text{Sign}(S_i)$  equals -1 if  $S_i$  is negative.  $J_{\alpha\alpha}$ ,  $J_{\beta\beta}$  and  $J_{\alpha\beta}$  are  $\alpha$ - $\alpha$ ,  $\beta$ - $\beta$ , and  $\alpha$ - $\beta$  interfacial energies, respectively.

In iteration, the kinetic energy of the aggregate is adjusted by the Monte Carlo technique. First, a lattice site and a site index are chosen at random. The index of the chosen site is then changed to the new index if the corresponding total system energy,  $H$ , does not increase. After each attempted index change, the Monte Carlo step increases, and a simulated mesostructure is yielded. Fig. 2 is a 3-dimensional simulated mesostructure plot of the cylinder specimen that involves 148,500 lattices. Different types of aggregates are composed of certain numbers of lattices, and between the aggregates are the interfaces or cement pastes.



Fig.1 Specimen lattice Plot



Fig.2 Specimen aggregate distribution

#### 4 Model Description

Simulations of the static tests were performed using the finite element analysis code, which was developed for static analysis of nonlinear structural systems. The Drucker-Prager criterion and the low tensile strength criterion are used. Based on comparison of the experimental and numerical results, the strength ratio between the cement paste (including interface) and coarse aggregate was randomly distributed between 0.1 to 0.4. Table 1 is the parameter used in the analysis.

Table 1 Parameters for coarse aggregate\*

Young's Modulus	Poisson's Ratio	Maxi. Tensile Stress	Maxi. Compressive Stress	Cohesion
17 MPa	0.167	20 MPa	100 Mpa	22.4 MPa

\*Strength ratio between cement paste (including interface) and aggregate: 0.1-0.4 randomly.

An 8-node isoparameter 3-dimensional element was used. In this case, there were 148,500 lattices in the cylinder model and each of them possessed different mechanical properties, such as ultimate strength and modulus of elasticity, which need to be incorporated in numerical analyses. However, it is very difficult or almost impossible to treat that many elements in finite element analysis due to the low efficiency and floating point errors of the

calculation. The situation becomes even more difficult with nonlinear analysis.

Modified Gauss point method has been successfully used to reduce the computer processing time while still guaranteeing accuracy ( Wang and Chen ,1997). The basic idea of the modified Gauss point method used here is that each Gauss point in the numerical integration corresponds to one lattice and, therefore, one element will involve a specific number of lattices, say 8 or 27 in a 3-dimensional problem. The Gauss point coordinates and the corresponding weight coefficients need to be modified because of the evenly distributed lattices. Table 2 lists the values of Gauss point coordinates,  $\xi_i$ , and the weighted coefficient,  $H_i$  for the different number of Gauss points,  $n$ , evenly distributed between  $-1$  and  $+1$  in case of 1-dimensional.

Table 2 Values of  $\xi_i$  corresponding to various  $n$

n	$H_i$	$\xi_i$	Precise for $m^{\text{th}}$ Order Polynomial
3	2/3	$\pm 0.707107$ 0.0	$m=3$
4	2/4	$\pm 0.794654$ $\pm 0.187593$	$m=4$ or 5
5	2/5	$\pm 0.832497$ 0.0 $\pm 0.374541$	$m=5$
6	2/6	$\pm 0.866246$ $\pm 0.422522$ $\pm 0.374541$	$m=5$ or 6

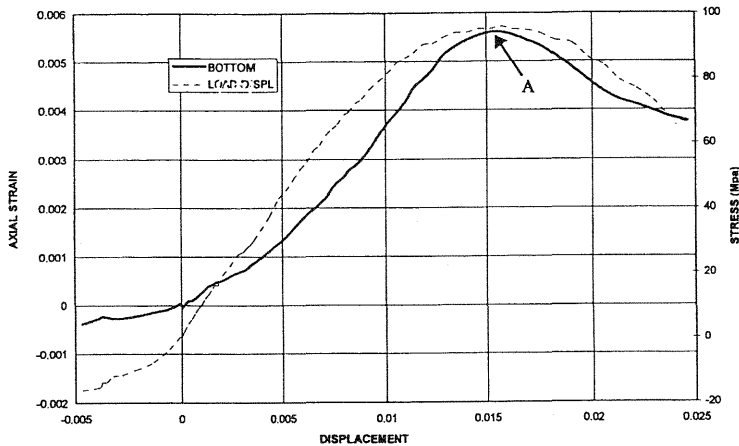


Fig.3(a) Typical displacement-stress relationship of experimental data (Units of displacement is in cm)

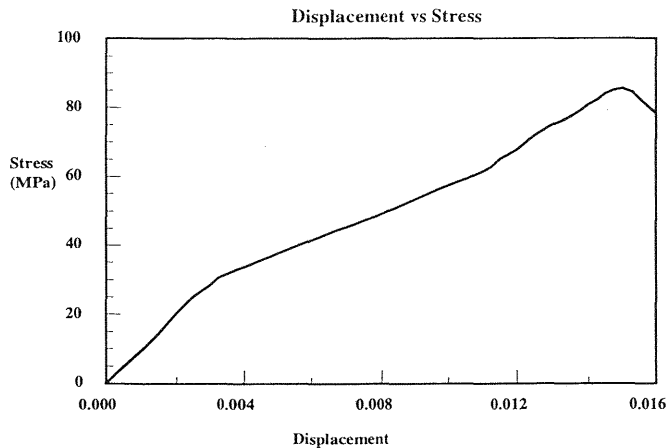
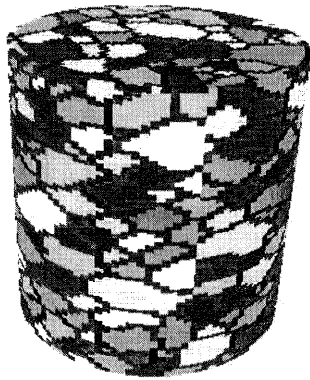


Fig.3(b) Typical displacement-stress relationship of numerical simulation (Units of displacement is in cm)

In this paper, 27 modified Gauss points or lattices were involved in one 8-node element. Therefore, the cylinder specimen had 5,500 elements, which stand for 148,500 lattices. Several typical examples (Wang and Chen, 1997) show that the modified Gauss point method not only reduces the calculating time greatly but also guarantees the accuracy of the computation.

## 5 Results and Discussion

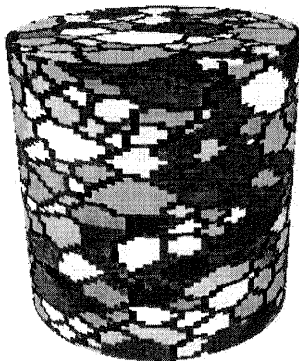
Results of the experimental measurements and numerical analyses are shown in Fig. 3 through 5. Very good agreement is found between displacement and stress (Fig. 3(a, b)). Fig. 4(a) shows the failure specimens by test, while Fig. 4(b) shows the damaged cylinders by numerical simulation at various confining pressures. Fig. 5 represents comparison of the angles of the failure planes by experimental and numerical analyses. It shows that a distinct failure surface or surfaces change orientation from vertical to angled as confinement increases. Based on this research, there are several points that need to be emphasized. First, confining pressure due to friction between platen and specimen has a predominating effect on the failure angle of a specimen under triaxial loading. It is essential to relieve the friction between the platens and the specimens. Second, to predict the failure mechanism accurately, randomly distributed cement paste and coarse aggregate is necessary in the simulation of 3-dimensional concrete specimen under triaxial loading.



P = 0.0 Mpa



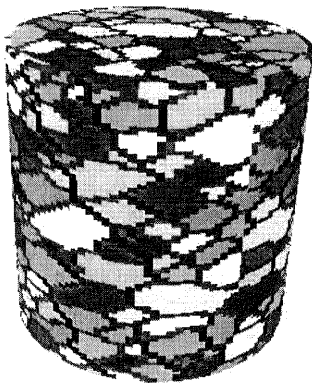
P = 1.7 Mpa



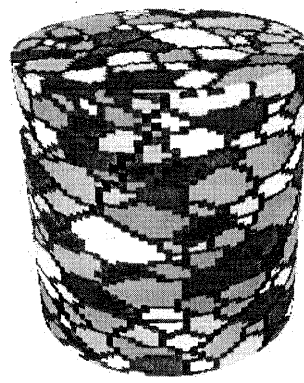
P = 3.5 Mpa



P = 7.0 Mpa



P = 14.0 Mpa



P = 28.0 Mpa

Fig.4(b) Damaged specimen by numerical simulation

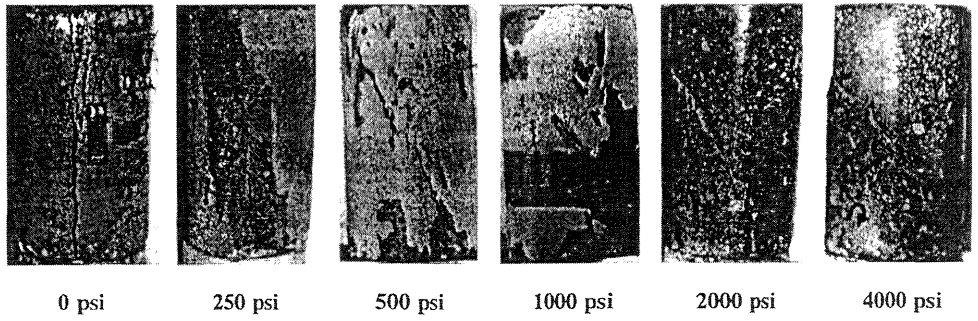


Fig.4(a). Damaged specimen by experiments

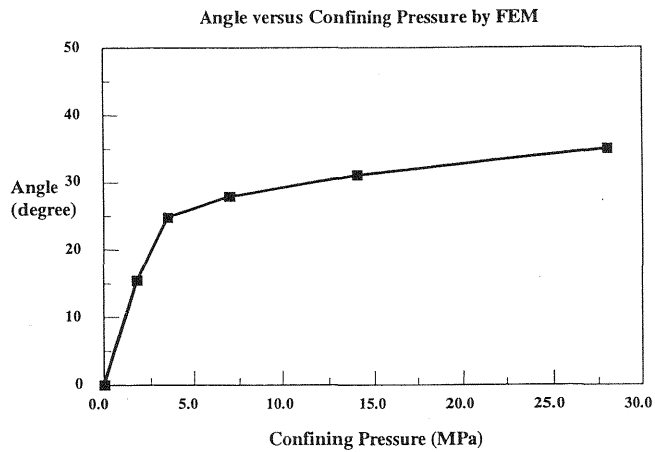
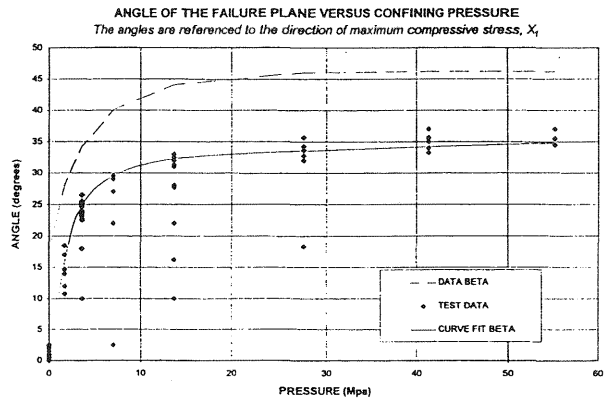


Fig.5. Angle versus confining pressure by test(a) and numerical simulation(b)

## 6 Conclusion

This study presented a procedure to predict the failure mechanisms of concrete under triaxial loading. Both experimental and numerical studies showed changes in the orientation of the failure plane as confining pressure increased for concrete cylinder specimens. For realistic triaxial loading in experiments, it is essential to relieve the friction between the platen and specimen. Based on comparison of experimental and numerical results, the strength ratio between cement paste (including interface) and coarse aggregate is randomly distributed between 0.1 to 0.4. It is strongly suggested that a realistic 3-dimensional meso-structure simulation be used in a numerical model. The presented modified Gauss point method is a key step to guarantee the efficiency and accuracy of the simulation.

## 7 References

- Desiderio, K. (1996) Grain size distributions and strength variability of high-purity alumina. **J. Am. Ceram. Soc.**, 79(2)305-12.
- Hockin, H. K. (1996). Influence of grain size on the grinding response of alumina. **J. Am. Ceram. Soc.**, 79(5)1307-13.
- Hassold, G. N. (1990). Computer simulation of final-stage sintering: I model, kinetic, and microstructure. **J. Am. Ceram. Soc.**, 73(10).
- Gerstle, K. H. (1980) Behavior of concrete under multiaxial stress states. **J. Eng. Mech. Division**, ASCE, 1383-1403
- Murrell, S.A. (1965) The effect of triaxial stress systems on the strength of rocks at atmospheric temperatures. **Geophys. J. R. Astron Soc.** 10, 231-281.
- Palaniswamy, R. (1972) Deformation and failure of hardened cement paste subjected to multiaxial stress. **Proc. of the RILEM**, 169-179.
- Wang, M. L. and Chen, Z. L. (1997). Modified Gauss point method and its application in THMs. **Proc. of Computer Aided Design of High-Temperature Materials**, Sante Fe, New Mexico, USA.
- Wang, M. L. and Rutland, C.A.(1995). Strain measurements using real time X-ray images, **Journal of British Society for Strain Measurement**, 'Strain' 87-94
- Wawersik, W.R. (19970) Post-failure behavior of a granite and diabase. **Rock Mechanics**, 3, 61-85
- Zimmerman, R.M. (1977) Strength and deformation response of concrete under multiaxial loadings-cooperative project. **Final Report ENG 74-12097** for NSF.